06

Second-harmonic generation in the surface layer of a dielectric spheroidal particle: II. Analysis of the solution

© A.A. Shamyna, V.N. Kapshai¶, A.I. Talkachov¶¶

Francisk Skorina Gomel State University,
246019 Gomel, Belarus

e-mail: anton.shamyna@gmail.com, ¶kapshai@rambler.ru, ¶¶anton.talkachov@gmail.com

Received February 5, 2022
Revised April 18, 2022
Accepted May 2, 2022

The vectors used in the solution of the problem of second-harmonic generation in the surface layer of a dielectric spheroidal particle are explicitly expressed in terms of the basis vectors of the spherical, cylindrical, and Cartesian coordinate systems. Three-dimensional directivity patterns characterizing the spatial distribution of the generated radiation in the far-field region and its polarization are constructed. It is found that for a small size of a spheroidal particle, the directivity pattern due to each of the non-chiral components of the nonlinear dielectric susceptibility tensor has its own individual shape. A proportional increase in the linear dimensions of the particle leads to separation of several directions of predominant radiation with a high directivity in the directivity pattern. If the exciting radiation has a linear polarization, then the generated radiation due to one (any) of the independent components of the tensor is also linearly polarized. Mathematical properties characterizing the spatial distribution of the generated radiation in the far-field region and properties associated with the change of problem parameters are found for the functions used in the solution. A relationship between the symmetries of the directivity patterns of doubled-frequency radiation and the indicated properties is revealed. The conditions under which the generation of radiation does not occur and the conditions under which the generated radiation has a linear polarization are found. The above conditions are related to the features of the spatial distribution of the generated radiation and its polarization, illustrated in the directivity patterns. Methods for estimating the independent components of the nonlinear dielectric susceptibility tensor using these conditions are proposed.

Keywords: second-harmonic generation, spheroidal dielectric particle, symmetry of the spatial distribution of radiation, conditions for the absence of generation, conditions for the generation of linearly polarized radiation.

DOI: 10.21883/EOS.2022.07.54727.3229-22

Explicit form of vectors

The resulting formulae in the considered problem are hard to analyze, since they are rather cumbersome. To obtain additional information regarding the studied phenomenon, we illustrate the spatial distribution of generated radiation with directivity patterns, which allow one both to identify the preferred radiation directions and to analyze the polarization of generated waves.

Let us direct Cartesian axes in such a way that the wave vector of an incident electromagnetic wave lies in plane OXZ, the spheroidal particle axis is aligned with axis OZ, and the geometric particle center is at the origin of coordinates. The diagrams of the problem being solved is similar in this case to the diagram of second-harmonic generation in the surface layer of a cylindrical particle [1], and formulae for the explicit form of vectors similar to the ones found in [2] may be used:

$$\mathbf{k}^{(\omega)} = k_\omega \sin\theta_{\text{in}}\mathbf{e}_x + k_\omega \cos\theta_{\text{in}}\mathbf{e}_z, \quad \mathbf{k}^{(2\omega)} = k_{2\omega}\mathbf{e}_r,$$

$$\mathbf{e}^{(\omega)} = \frac{\cos\theta_{\text{in}}(-\cos\varphi_{\text{in}} + i\sigma\sin\varphi_{\text{in}})}{\sqrt{1+\sigma^2}}\,\mathbf{e}_x + \frac{(-i\sigma\cos\varphi_{\text{in}} - \sin\varphi_{\text{in}})}{\sqrt{1+\sigma^2}}\,\mathbf{e}_y + \sin\theta_{\text{in}}\frac{\cos\varphi_{\text{in}} - i\sigma\sin\varphi_{\text{in}}}{\sqrt{1+\sigma^2}}\,\mathbf{e}_z. \quad (1)$$

Here, θ_{in} is the angle between wave vector $\mathbf{k}^{(\omega)}$ and the positive direction of axis OZ, k_ω and $k_{2\omega}$ are the moduli of wave vectors $\mathbf{k}^{(\omega)}$ and $\mathbf{k}^{(2\omega)}$, respectively, φ_{in} is the angle between plane OXZ and the major semiaxis of the polarization ellipse, and σ is the ellipticity of an incident wave (ratio of the minor semiaxis of the polarization ellipse to the major semiaxis).

The scattering vector components may be calculated using the following formulae:

$$q_z = \mathbf{e}_z(2\mathbf{k}^{(\omega)} - \mathbf{k}^{(2\omega)}) = 2k_\omega(\cos\theta_{\text{in}} - \xi\cos\theta),$$

$$\mathbf{q}_\perp = (1 - \mathbf{e}_z \otimes \mathbf{e}_z)(2\mathbf{k}^{(\omega)} - \mathbf{k}^{(2\omega)}) = -2k_\omega\left[(\xi\sin\theta - \sin\theta_{\text{in}}\cos\varphi)\mathbf{e}_\rho + \sin\theta_{\text{in}}\sin\varphi\mathbf{e}_\varphi\right],$$

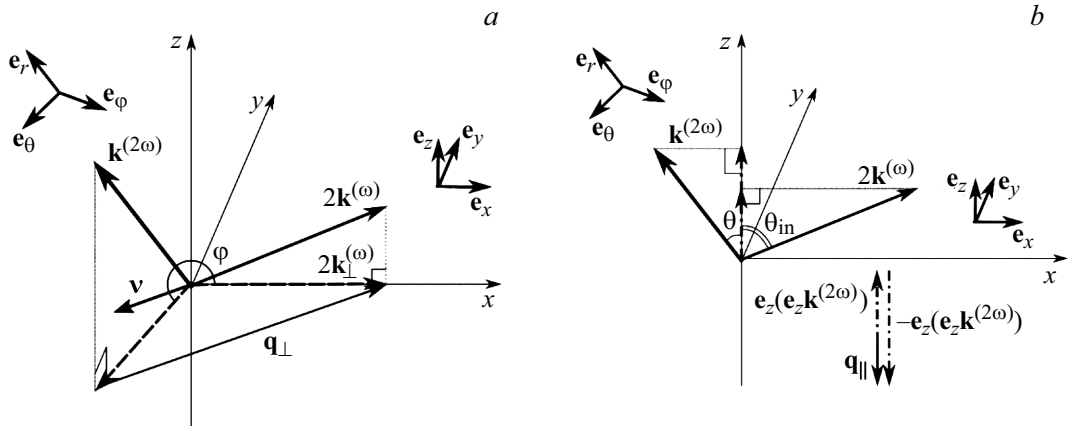

Figure 1. Schematic arrangement of vectors used in solving the problem of second-harmonic generation in the surface layer of a spheroidal particle: (a) vectors in plane OXY, (b) vectors along axis OZ.

$$q_\perp = |\mathbf{q}_\perp| = 2k_\omega \sqrt{\sin^2\theta_{in} - 2\xi \sin\theta_{in}\sin\theta\cos\varphi + \xi^2\sin^2\theta}, \quad (2)$$

where $(\mathbf{e}_\rho, \mathbf{e}_\varphi, \mathbf{e}_z)$ are cylindrical coordinate vectors and (r, θ, φ) are spherical coordinates. Coefficient ξ characterizes the dispersion associated with radiation frequency doubling and is calculated as

$$\xi = \frac{k_{2\omega}}{2k_\omega} = \frac{n_{2\omega}}{n_\omega}. \quad (3)$$

A unit vector directed along $\mathbf{q}_\perp$ may be represented in mathematical terms by the following expression:

$$\boldsymbol{\nu} = \frac{\mathbf{q}_\perp}{q_\perp} = \frac{(-\xi\sin\theta + \sin\theta_{in}\cos\varphi)\mathbf{e}_\rho - \sin\theta_{in}\sin\varphi\mathbf{e}_\varphi}{\sqrt{\sin^2\theta_{in} - 2\xi\sin\theta_{in}\sin\theta\cos\varphi + \xi^2\sin^2\theta}}. \quad (4)$$

The schematic arrangement of vectors is presented in Fig. 1.

Directivity patterns

Notation

The notation used in plotting the patterns is similar to the one from [2–5]. It is assumed in all directivity patterns that a particle is located at the origin of coordinates. The distance from the origin of coordinates to the surface of the directivity pattern is directly proportional to the modulus of the Umov–Poynting vector of second-harmonic radiation in the corresponding direction. The longest lobes of the directivity pattern are aligned with the preferred radiation directions (e.g., the power radiated into the half-space of positive values on axis OX in Fig. 2, a exceeds the power radiated in the opposite direction). All patterns are normalized to the maximum radiation power density. Curves on the surface of a directivity pattern characterize the orientation of the polarization ellipse of double-frequency radiation: solid curves are aligned with major semiaxes of polarization ellipses, while dashed curves are aligned with minor semiaxes.

Solid arrows denote the orientation of the wave vector of an incident electromagnetic wave (e.g., the vector is directed along axis OX in Fig. 2, a). The major semiaxis of the polarization ellipse of excitation radiation is coincident with the dashed arrow in directivity patterns (this arrow is aligned with axis OZ in Fig. 2, a).

Grayscale diagrams located in the right $(-\pi/2 < \varphi < \pi/2)$ and left $(\pi/2 < \varphi < 3\pi/2)$ upper corners of a directivity pattern are the projections of this directivity pattern onto the forward and the backward hemispheres, respectively (see Fig. 3, g). White and black colors correspond to the maximum and the minimum power density, respectively. The legend is shown in the left part of Fig. 3, *f*.

According to the same projection diagram, grayscale diagrams located in the right and left lower corners of a directivity pattern characterize the polarization of generated radiation. White ($\sigma = +1$, right-hand polarization) and black ($\sigma = -1$, left-hand polarization) colors correspond to circularly polarized radiation. The legend is shown in the right part of Fig. 3, *f*.

Analysis of directivity patterns

An exhaustive analysis of the dependence of the spatial distribution of generated radiation on the parameters of a particle and excitation radiation for all parameter combinations is a rather time-consuming task, since a considerable number of parameters are adjusted ($\chi^{(2)}_{1-4}$, $k_\omega a_x$, ρ, θ_{in}, φ_{in}, σ, ξ). Therefore, only a few of the observed trends are illustrated in the present study. The value of $\xi = 1.34/1.33$, which corresponds to the refraction indices of water at radiation wavelengths of 425 and 850 nm, was used to plot all the directivity patterns presented below.

Figures 2, a–d illustrate the power density distribution of generated radiation for a small-sized particle $(k_\omega a_x = 0.1)$ shaped as a prolate $(\rho = 1.5)$ ellipsoid of revolution for each of the independent components

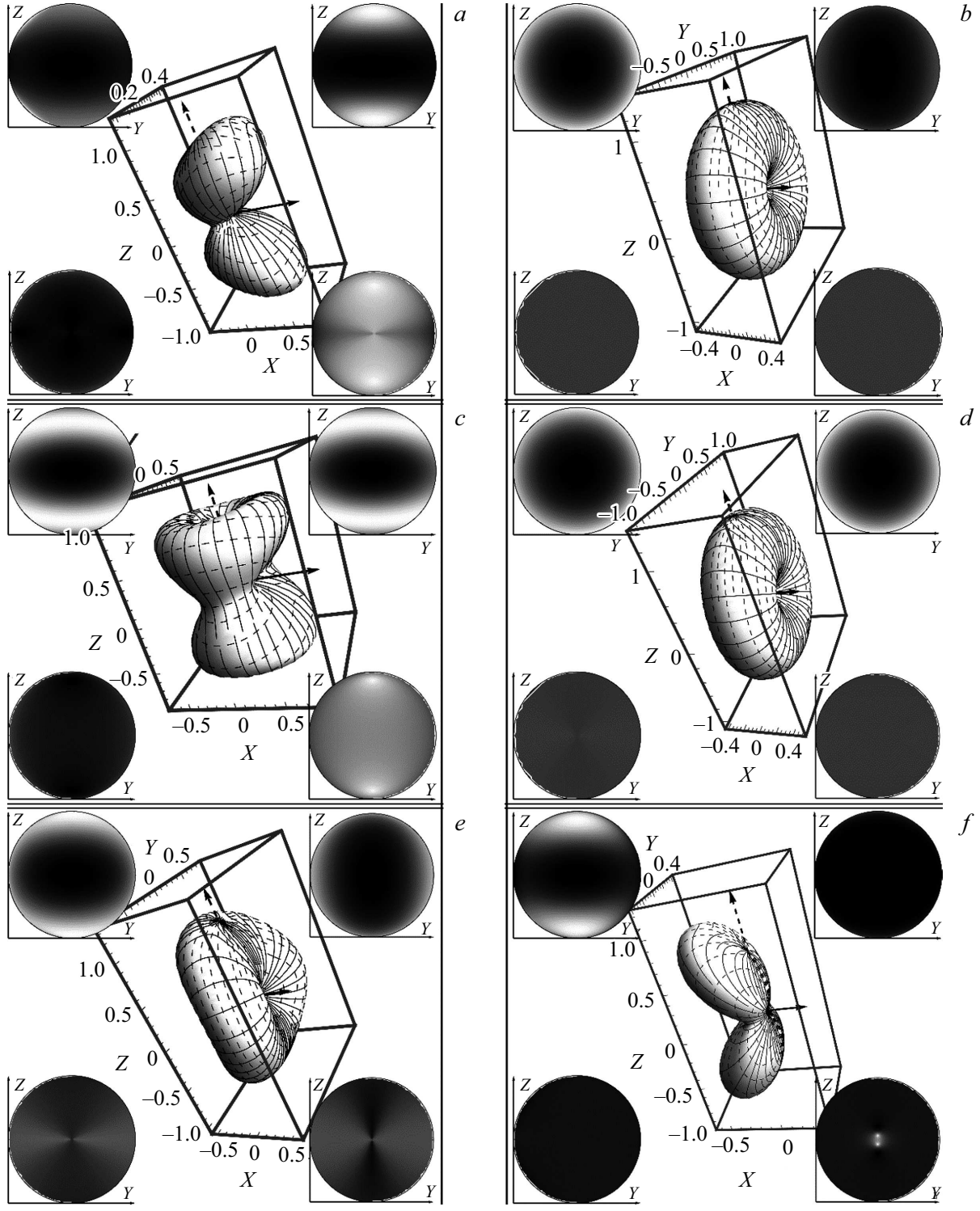

Figure 2. Directivity patterns for a small-sized dielectric particle at $k_\omega a_x = 0.1$, $\sigma = 0.5$, $\theta_{\text{in}} = \pi/2$, $\varphi_{\text{in}} = 0$. The other parameter values are as follows: (*a*) $\chi_1^{(2)} \neq 0$, $\chi_{2-4}^{(2)} = 0$, $\rho = 1.5$, (*b*) $\chi_2^{(2)} \neq 0$, $\chi_{1,3,4}^{(2)} = 0$, $\rho = 1.5$, (*c*) $\chi_3^{(2)} \neq 0$, $\chi_{1,2,4}^{(2)} = 0$, $\rho = 1.5$, (*d*) $\chi_4^{(2)} \neq 0$, $\chi_{1-3}^{(2)} = 0$, $\rho = 1.5$, (*e*) $\chi_1^{(2)} = -0.627$, $\chi_2^{(2)} = 0.778$, $\chi_3^{(2)} = -0.021$, $\chi_4^{(2)} = 0$, $\rho = 1.5$, (*f*) $\chi_4^{(2)} \neq 0$, $\chi_{1-3}^{(2)} = 0$, $\rho = 1$.

of the tensor of nonlinear dielectric susceptibility $\chi_{ijk}^{(2)}$ (i.e., with only one of the $\chi_{1-4}^{(2)}$ components differing from zero). The parameter values correspond to vector $\mathbf{k}^{(\omega)}$ directed perpendicular to the dielectric particle axis ($\theta_{\text{in}} = \pi/2$) and the right-hand elliptical polarization of excitation radiation ($\sigma = 0.5$) with the major semiaxis aligned with the particle symmetry axis ($\varphi_{\text{in}} = 0$).

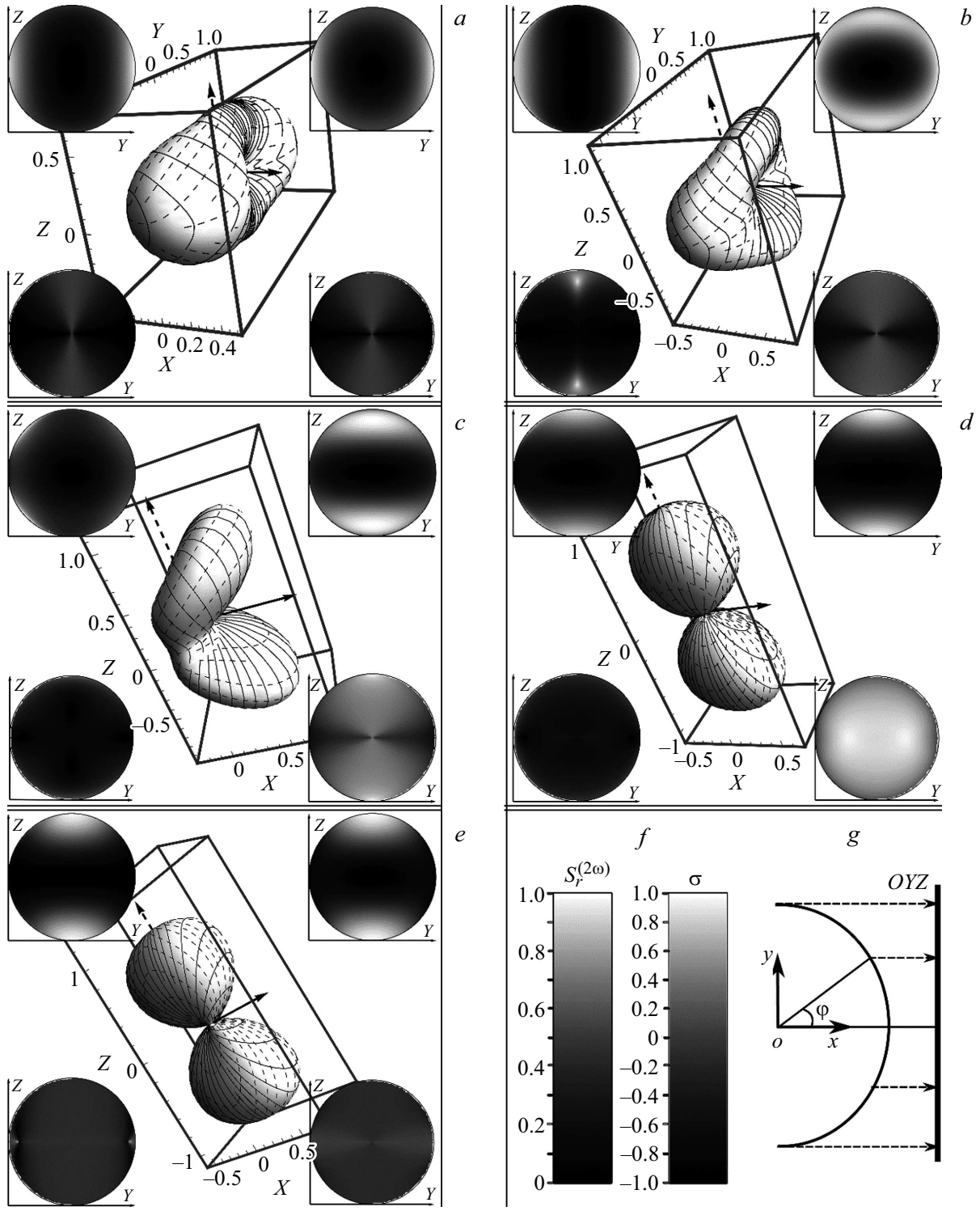

Figure 3. Directivity patterns characterizing the dependence of the spatial distribution of the second-harmonic field on the ratio of semiaxes of a spheroidal particle at $\chi_1^{(2)} \neq 0$, $\chi_{2-4}^{(2)} = 0$, $k_\omega a_x = 0.1$, $\sigma = 0.5$, $\theta_{\text{in}} = \pi/2$, $\varphi_{\text{in}} = 0$. The ratios of semiaxes of a dielectric particle are (*a*) $\rho = 0.1$, (*b*) $\rho = 0.5$, (*c*) $\rho = 1.1$, (*d*) $\rho = 2$, (*e*) $\rho = 10$. The legend is shown in panel *f*, and the projection diagram is presented in panel *g*.

It can be seen that a specific shape of the directivity pattern corresponds to each non-chiral anisotropy coefficient $(\chi_{1-3}^{(2)})$ in the case of a small-sized particle. If $\chi_1^{(2)} \neq 0$, $\chi_{2-4}^{(2)} = 0$ (Fig. 2, *a*) or $\chi_3^{(2)} \neq 0$, $\chi_{1,2,4}^{(2)} = 0$ (Fig. 2, *c*), waves with right-hand and left-hand polarizations are radiated into the forward and backward hemispheres, respectively.

The directivity pattern for $\chi_2^{(2)} \neq 0$, $\chi_{1,3,4}^{(2)} = 0$ (Fig. 2, *b*) shows that generated radiation has linear polarization in all directions.

The directivity pattern plotted at $\chi_{1-4}^{(2)}$ values corresponding to malachite green dye, which had its independent components of the tensor of nonlinear dielectric susceptibility determined in [6], is presented in Fig. 2, *e*. The similarity between the patterns in Figs. 2, *b* and 2, *e* in directions close to plane *OXY* is attributable to the fact that the generated radiation intensity due to component $\chi_2^{(2)}$ (Fig. 2, *b*) dominates over the radiation intensity associated with $\chi_1^{(2)}$ (Fig. 2, *a*) at $\chi_1^{(2)}$ and $\chi_2^{(2)}$ values of the same order. In the other directions, the distribution pattern of second-harmonic radiation is shaped by the interference of double-frequency electromagnetic waves produced by components $\chi_1^{(2)}$ and $\chi_2^{(2)}$.

The similarity of the spatial distributions of radiation in Figs. 2, *b* and 2, *d*, which correspond to $\chi_2^{(2)} \neq 0$, $\chi_{1,3,4}^{(2)} = 0$ and $\chi_4^{(2)} \neq 0$, $\chi_{1-3}^{(2)} = 0$, is also evident. The difference consists in the fact that the radiation polarization in Fig. 2, *d* differs from a linear one in the upper and lower parts of the pattern. No such similarity was observed in the case of generation in the surface layer of a spherical particle [3]. At $\rho = 1$, which corresponds to a spherical particle shape, the directivity pattern for $\chi_4^{(2)} \neq 0$, $\chi_{1-3}^{(2)} = 0$ (Fig. 2,*f*) differs considerably from the one for $\chi_2^{(2)} \neq 0$, $\chi_{1,3,4}^{(2)} = 0$, which is similar in shape to the pattern in Fig. 2, *b*. In fact, a thorough analysis revealed that the spatial distribution of generated radiation for $\chi_4^{(2)} \neq 0$, $\chi_{1-3}^{(2)} = 0$ is also close to the distribution for $\chi_2^{(2)} \neq 0$, $\chi_{1,3,4}^{(2)} = 0$ at other values of ρ (i.e., values differing from unity).

The probable reason behind these trends is as follows. In the case of a small-sized dielectric particle, the dominant term shaping the spatial distribution of generated radiation for a chiral layer ($\chi_4^{(2)} \neq 0$, $\chi_{1-3}^{(2)} = 0$) is canceled out at $\rho \to 1$ (see Part I of the present study). The directivity pattern is then shaped by the term of a higher order of smallness (second-order spherical Bessel function in [3]). The slight deviation of polarization from a linear one in the upper and lower parts of the pattern is attributable exactly to this influence of terms of a higher order of smallness: the left-hand radiation polarization in Fig. 2,*f* matches the left-hand polarization corresponding to the upper and lower parts of the directivity pattern in Fig. 2, *d*.

The influence of coefficient ρ on the nature of the spatial distribution of generated radiation at a small size of a dielectric particle and independent components $\chi_1^{(2)} \neq 0$, $\chi_{2-4}^{(2)} = 0$ of the tensor of nonlinear dielectric susceptibility is illustrated by Fig. 3.

If a dielectric particle is shaped as an oblate ellipsoid of revolution (Fig. 3, *a, b*), radiation is generated primarily in the directions perpendicular to the plane in which the wave vector of excitation radiation and the particle axis lie. At $\rho = 0.1$ (Fig. 3, *a*), the polarization of double-frequency radiation tends to be opposite to the polarization of an incident electromagnetic wave.

If a dielectric particle is prolate (Fig. 3, *d, e*), radiation is generated primarily in the plane in which the wave vector of an incident wave and the particle axis lie. The polarization of generated radiation tends to be left-handed when the values of ρ are large (Fig. 3, *e*).

At ρ values close to unity (Fig. 3, *c*), the shape of the directivity pattern is similar to the one typical of generation in the surface layer of a spherical particle [3]. Radiation with its polarization matching the one of an incident wave is then generated into the forward hemisphere, and radiation with the opposite polarization is generated into the backward hemisphere.

The spatial distribution of generated radiation depends directly on the polarization of an incident electromagnetic wave. Figures 4, *a, b* present the directivity patterns plotted for independent components $\chi_1^{(2)} \neq 0$, $\chi_{2-4}^{(2)} = 0$ of the tensor of nonlinear dielectric susceptibility at linear ($\sigma = 0$) and right-hand circular ($\sigma = 1$) polarizations of excitation radiation. It can be seen that linearly polarized double-frequency radiation is generated upon the incidence of a linearly polarized wave onto a dielectric particle. It is easy to verify that this trend persists when an optically nonlinear layer is purely chiral ($\chi_4^{(2)} \neq 0$, $\chi_{1-3}^{(2)} = 0$) or purely non-chiral ($\chi_{1-3}^{(2)} \neq 0$, $\chi_4^{(2)} = 0$). If a circularly polarized wave is incident on a particle, elliptically polarized second-harmonic radiation (with the ellipticity depending on directions θ, φ) is generated. An intermediate case is illustrated by the directivity pattern in Fig. 3, *d* with $\sigma = 0.5$. Comparing it to the case presented in Fig. 4, *c* with $\sigma = -0.5$, one can see that the polarizations of radiation generated in the same direction at $\sigma = 0.5$ and $\sigma = -0.5$ are opposite, while the amplitude remains constant. These features persisted in second-harmonic generation in the surface layer of spherical [3] and cylindrical [2] dielectric particles.

The polarization of excitation radiation is also of significance at $\chi_3^{(2)} \neq 0$, $\chi_{1,2,4}^{(2)} = 0$. Linearly polarized radiation is generated upon the incidence of linearly polarized radiation ($\sigma = 0$) onto a dielectric particle (Fig. 4, *d*). If an incident electromagnetic wave has the right-hand circular polarization ($\sigma = 1$), elliptically polarized second-harmonic radiation is generated (Fig. 4, *e*). When the polarization of excitation radiation is switched to the opposite one ($\sigma = -1$), the polarization of double-frequency radiation also switches (Fig. 4,*f*), while the intensity remains unchanged.

It was noted in [2–5,7,8] that the size of a dielectric particle has a considerable effect on the distribution of second-harmonic radiation in the far-field region. A similar dependence is typical of generation in the surface layer of spheroidal particles. Figures 5, *a, b* (at $\chi_1^{(2)} \neq 0$, $\chi_{2-4}^{(2)} = 0$) demonstrate that proportional scaling of linear dimensions of a dielectric particles by a factor of 2 (from $k_\omega a_x = 0.5$ to $k_\omega a_x = 1.0$) resulted in the emergence of two preferred

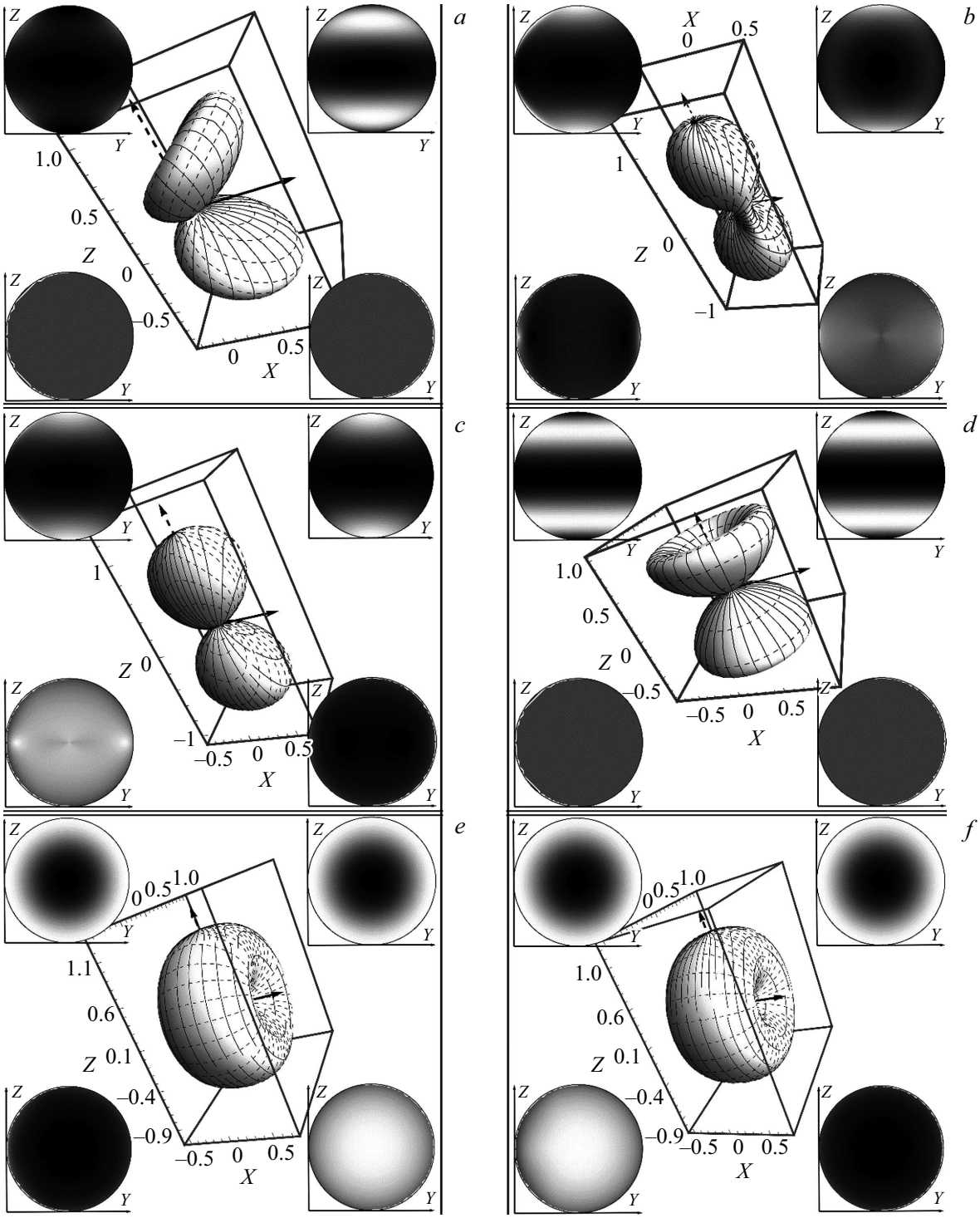

Figure 4. Directivity patterns characterizing the influence of polarization of an incident wave on the spatial distribution of generated radiation at $k_\omega a_x = 0.1$, $\rho = 2$, $\theta_{\text{in}} = \pi/2$, $\varphi_{\text{in}} = 0$. The other parameter values are as follows: (*a*) $\chi_1^{(2)} \neq 0$, $\chi_{2-4}^{(2)} = 0$, $\sigma = 0$, (b) $\chi_1^{(2)} \neq 0$, $\chi_{2-4}^{(2)} = 0$, $\sigma = 1$, (*c*) $\chi_1^{(2)} \neq 0$, $\chi_{2-4}^{(2)} = 0$, $\sigma = -0.5$, (*d*) $\chi_3^{(2)} \neq 0$, $\chi_{1,2,4}^{(2)} = 0$, $\sigma = 0$, (*e*) $\chi_3^{(2)} \neq 0$, $\chi_{1,2,4}^{(2)} = 0$, $\sigma = 1$, (*f*) $\chi_3^{(2)} \neq 0$, $\chi_{1,2,4}^{(2)} = 0$, $\sigma = -1$.

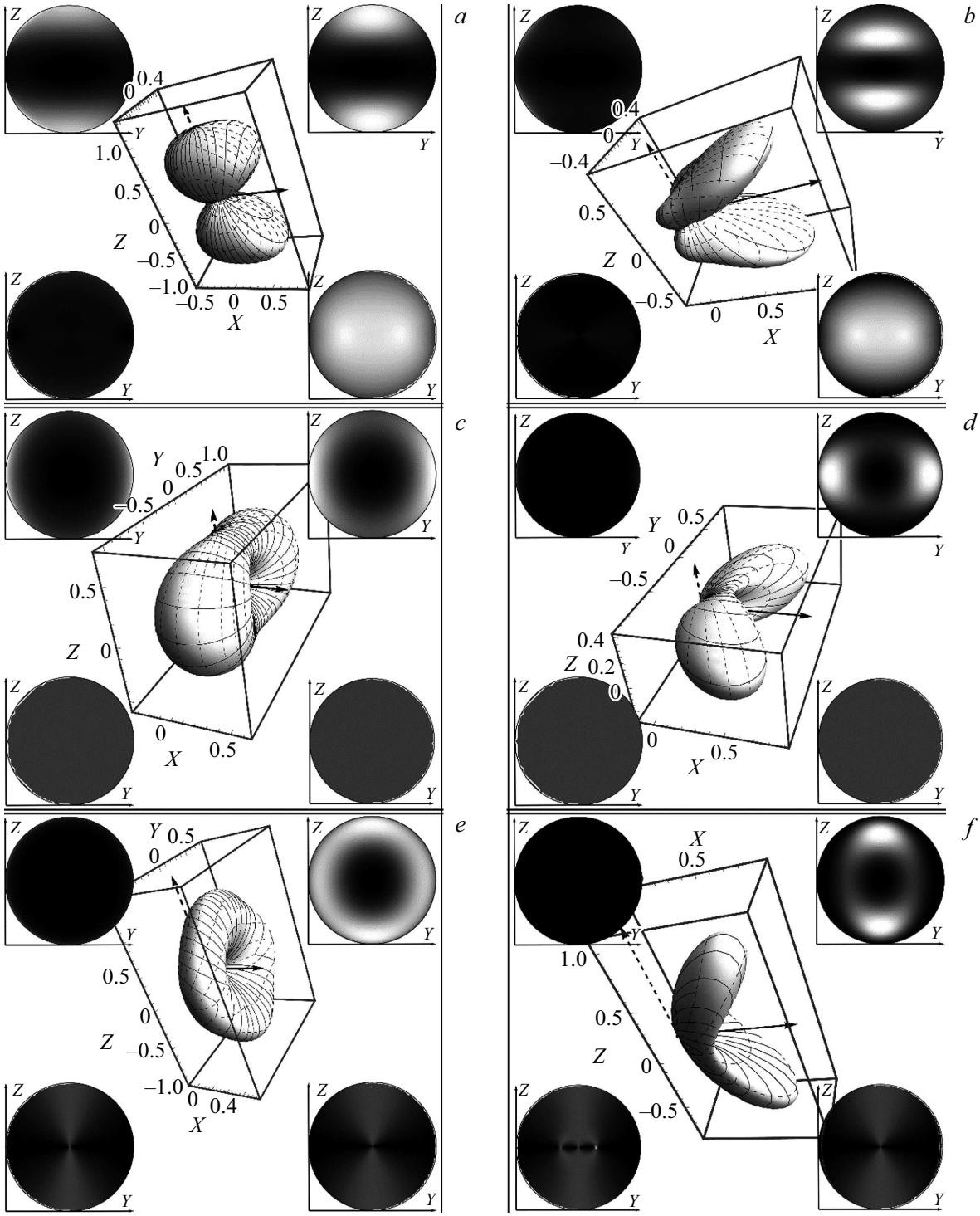

Figure 5. Directivity patterns characterizing the influence of linear dimensions of a dielectric particle on the spatial distribution of generated radiation at $\sigma = 0.5$, $\theta_{\text{in}} = \pi/2$, $\varphi_{\text{in}} = 0$. The other parameter values are as follows: (*a*) $\chi_1^{(2)} \neq 0$, $\chi_{2-4}^{(2)} = 0$, $\rho = 2$, $k_\omega a_x = 0.5$, (*b*) $\chi_1^{(2)} \neq 0$, $\chi_{2-4}^{(2)} = 0$, $\rho = 2$, $k_\omega a_x = 1.0$, (*c*) $\chi_2^{(2)} \neq 0$, $\chi_{1,3,4}^{(2)} = 0$, $\rho = 2$, $k_\omega a_x = 0.5$, (*d*) $\chi_2^{(2)} \neq 0$, $\chi_{1,3,4}^{(2)} = 0$, $\rho = 2$, $k_\omega a_x = 1.0$, (*e*) $\chi_1^{(2)} \neq 0$, $\chi_{2-4}^{(2)} = 0$, $\rho = 0.1$, $k_\omega a_x = 1.0$, (*f*) $\chi_1^{(2)} \neq 0$, $\chi_{2-4}^{(2)} = 0$, $\rho = 0.1$, $k_\omega a_x = 2.0$.

radiation directions. Both the incident wave and electromagnetic waves generated in these directions have right-hand polarizations. The same trend persists, to a certain extent, in the transition from size $k_\omega a_x = 0.1$ (Fig. 3, *d*) to size $k_\omega a_x = 0.5$ (Fig. 5, *a*). At $\chi_2^{(2)} \neq 0$, $\chi_{1,3,4}^{(2)} = 0$, two main lobes of the directivity pattern also form (this time in the plane perpendicular to the particle axis) when the particle dimensions increase by a factor of 2 (Fig. 5, *c, d*).

In the case of generation in the surface layer of a dielectric particle shaped as an oblate ($\rho = 0.1$, $\chi_1^{(2)} \neq 0$, $\chi_{2-4}^{(2)} = 0$) ellipsoid of revolution, main lobes of the directivity pattern emerging when the particle dimensions increase by a factor of 2 (Figs. 5, *e, f*) are, in contrast to the pattern in Fig. 5, *f* for $\rho = 2$, compressed in the direction perpendicular to the particle axis and the wave vector of excitation radiation. A similar emergence of preferred radiation directions with an increase in particle size was also observed in the case of nonlinear generation in the surface layer of spherical and cylindrical particles [3,4].

Note that the directivity patterns in all panels of Figs. 2–5 have two mirror symmetry planes (*OXZ* and *OYZ*). This is attributable to the presence of two corresponding mirror symmetry planes in the diagram of the problem.

In contrast to a spherical particle, a spheroidal particle features a distinguished symmetry axis; therefore, the orientation of the wave vector of an incident electromagnetic wave relative to the particle axis should also affect the spatial distribution of generated radiation. This effect is illustrated by Fig. 6.

Comparing Fig. 6, *a* with Fig. 5, *b*, one can see that the rotation of vector $\mathbf{k}^{(\omega)}$ at $\chi_1^{(2)} \neq 0$, $\chi_{2-4}^{(2)} = 0$ induces rotation of the upper main lobe of the directivity pattern in the same direction. The size of the lower main lobe decreases significantly in the process. If the wave vector of an incident wave is rotated further, the main lobes of the directivity pattern shift additionally (Fig. 6, *b*). Note that the directivity pattern also assumes axial symmetry (Fig. 6, *c*) in the case of circular polarization of excitation radiation ($\sigma = 1$) directed along the particle symmetry axis ($\theta_{\text{in}} = 0$). If $\chi_3^{(2)} \neq 0$, $\chi_{1,2,4}^{(2)} = 0$, the nature of variation of the directivity pattern induced by the $\mathbf{k}^{(\omega)}$ vector rotation (Figs. 6, *d–f*) is similar to the one observed at $\chi_1^{(2)} \neq 0$, $\chi_{2-4}^{(2)} = 0$.

The spatial distributions of second-harmonic radiation in all panels of Fig. 6 feature symmetry plane *OXZ*.

Owing to the axial symmetry of a dielectric particle, the shape of the directivity pattern is affected not only by the orientation of the wave vector of excitation radiation, but also by the orientation of the polarization ellipse relative to the particle axis (polarization azimuth φ_{in}). This effect is illustrated by Fig. 7.

Comparing Figs. 7, *a, b* with Fig. 5, *a* ($\chi_1^{(2)} \neq 0$, $\chi_{2-4}^{(2)} = 0$), one may note that the main lobes of the directivity pattern rotate together with the polarization ellipse of excitation radiation. A similar dependence is also observed (see Figs. 7, *c–e*) for independent components $\chi_4^{(2)} \neq 0$, $\chi_{1-3}^{(2)} = 0$ of the tensor of nonlinear dielectric susceptibility in the case of incidence of linearly polarized radiation ($\sigma = 0$) on a particle. Mirror symmetry with respect to plane *OXY* is manifested in Figs. 7, *b, c, e*. The directivity patterns in Figs. 7, *a, d* are characterized by a twofold rotation axis of symmetry.

Properties of the spatial distribution of double-frequency radiation

Functions characterizing second-harmonic generation in the surface layer of dielectric particles shaped as an ellipsoid of revolution feature a number of mathematical properties related to the symmetry of the spatial distribution of generated radiation. Many of them are attributable to the symmetry of the problem diagram and match similar properties found for a cylindrical particle. All the properties listed in the present section hold true at arbitrary linear dimensions of a particle ($\forall a_x, \forall \rho$) and arbitrary values of the coefficient characterizing dispersion ($\forall \xi$).

We characterize mathematical properties using vector $\mathbf{f}^{(2\omega)}$, which is defined, following the notation from [1,3], as

$$\mathbf{f}^{(2\omega)} = X_{ijk}^{(2\omega)} e_j^{(\omega)} e_k^{(\omega)}, \tag{5}$$

where $X_{ijk}^{(2\omega)}$ is the effective susceptibility tensor calculated in accordance with formula (11) from Part I and $e_j^{(\omega)}$, $e_k^{(\omega)}$ are the components of unit polarization vector $\mathbf{e}^{(\omega)}$ of an incident electromagnetic wave.

The following properties of second-order nonlinear generation are the most general:

$$\begin{aligned}
&\mathbf{f}^{(2\omega)}(\theta + 2\pi m_1, \varphi + 2\pi m_2) = \mathbf{f}^{(2\omega)}(\theta, \varphi),\\
&\mathbf{f}^{(2\omega)}(-\theta, \varphi) = -(1 - 2\mathbf{e}_r \otimes \mathbf{e}_r)\mathbf{f}^{(2\omega)}(\theta, \varphi + \pi),\\
&S_r^{(2\omega)}(\theta + 2\pi m_1, \varphi + 2\pi m_2) = S_r^{(2\omega)}(\theta, \varphi),\\
&S_r^{(2\omega)}(-\theta, \varphi) = S_r^{(2\omega)}(\theta, \varphi + \pi).
\end{aligned} \tag{6}$$

Here and elsewhere, m, m_1, m_2 are arbitrary integer numbers. Similar properties have been found earlier in the analysis of second-harmonic generation and sum-frequency generation in surface layers of spherical and cylindrical dielectric particles [2–5]. They remain valid at any values of generation parameters ($\forall \chi_{1-4}^{(2)}, \forall \theta_{\text{in}}, \forall \varphi_{\text{in}}, \forall \sigma$), do not manifest themselves in directivity patterns of generated radiation, and are attributable to the features of trigonometric functions found in $\mathbf{f}^{(2\omega)}(\theta, \varphi)$ and $S_r^{(2\omega)}(\theta, \varphi)$.

If $\chi_2^{(2)}$ is the only nonzero independent component of the tensor of nonlinear dielectric susceptibility ($\chi_2^{(2)} \neq 0$, $\chi_{1,3,4}^{(2)} = 0$), the following is true at any values of the other

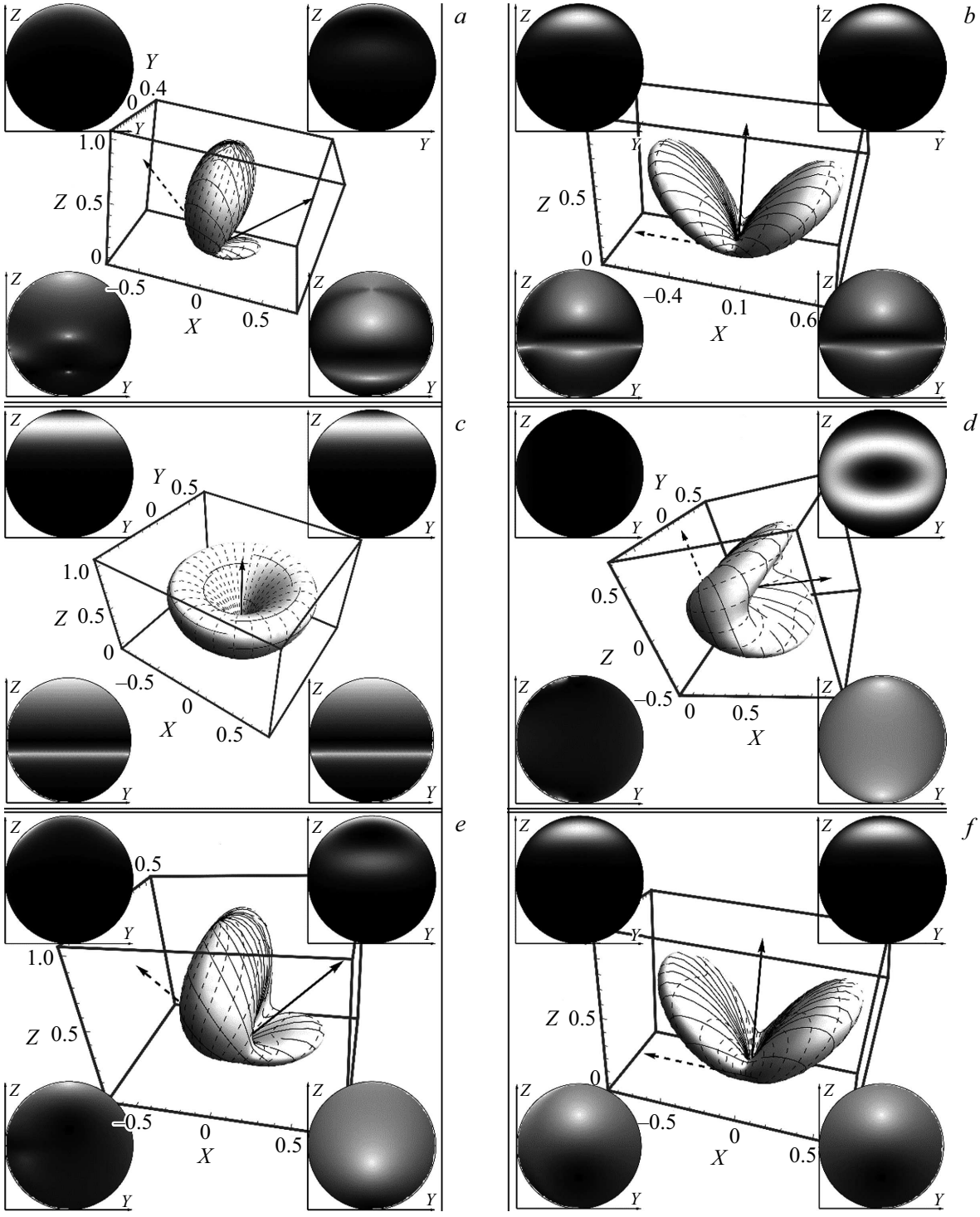

Figure 6. Directivity patterns characterizing the influence of orientation of the wave vector of an incident electromagnetic wave on the spatial distribution of generated radiation at $k_\omega a_x = 1.0$, $\rho = 2$, $\sigma = 0.5$, $\varphi_{\text{in}} = 0$. The other parameter values are as follows: (*a*) $\chi_1^{(2)} \neq 0$, $\chi_{2-4}^{(2)} = 0$, $\theta_{\text{in}} = \pi/4$, $\sigma = 0.5$, (*b*) $\chi_1^{(2)} \neq 0$, $\chi_{2-4}^{(2)} = 0$, $\theta_{\text{in}} = 0$, $\sigma = 0.5$, (*c*) $\chi_1^{(2)} \neq 0$, $\chi_{2-4}^{(2)} = 0$, $\theta_{\text{in}} = 0$, $\sigma = 1$, (*d*) $\chi_3^{(2)} \neq 0$, $\chi_{1,2,4}^{(2)} = 0$, $\theta_{\text{in}} = \pi/2$, $\sigma = 0.5$, (*e*) $\chi_3^{(2)} \neq 0$, $\chi_{1,2,4}^{(2)} = 0$, $\theta_{\text{in}} = \pi/4$, $\sigma = 0.5$, (*f*) $\chi_3^{(2)} \neq 0$, $\chi_{1,2,4}^{(2)} = 0$, $\theta_{\text{in}} = 0$, $\sigma = 0.5$.

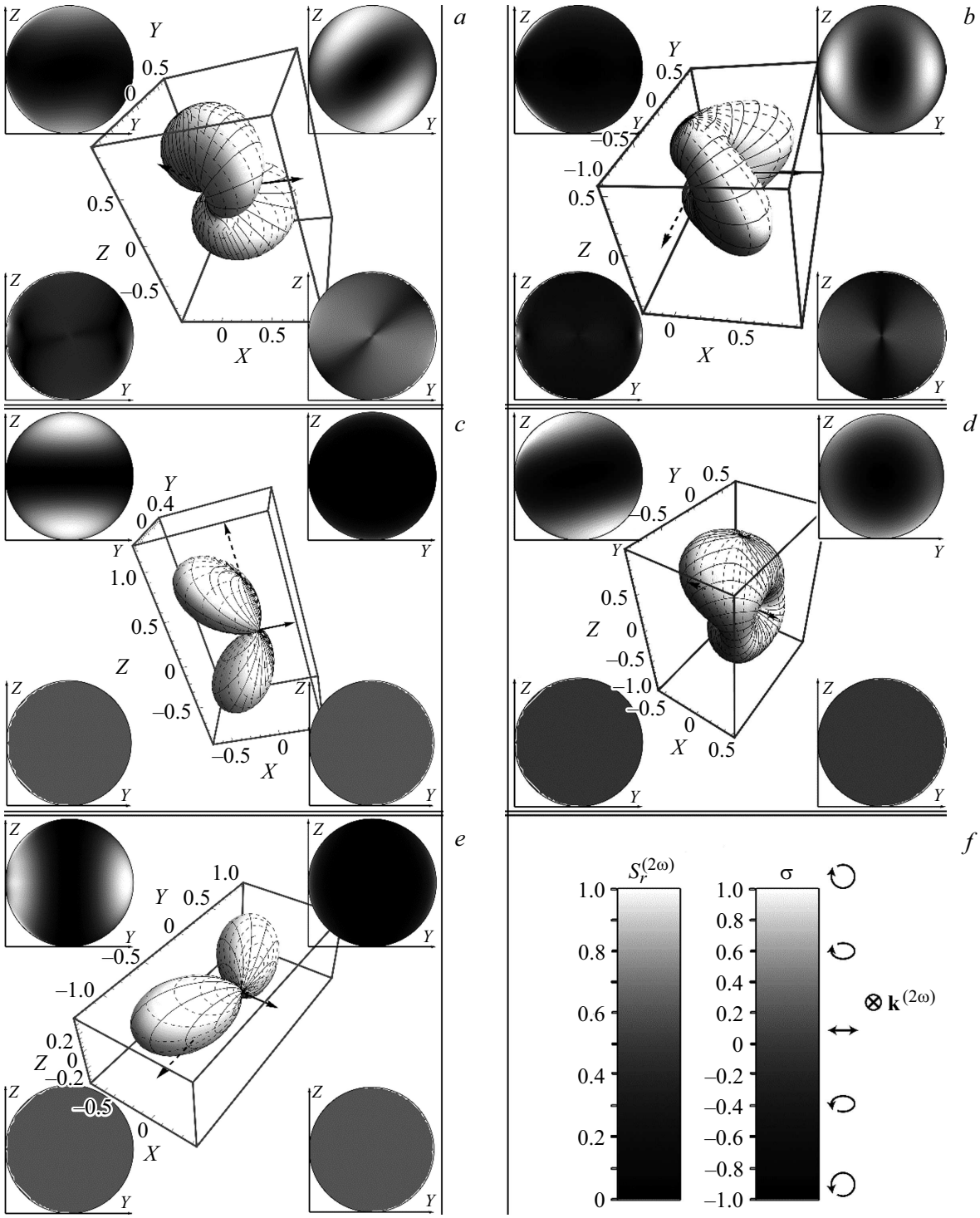

Figure 7. Directivity patterns characterizing the influence of orientation of the polarization ellipse of an incident electromagnetic wave on the spatial distribution of generated radiation at $k_\omega a_x = 0.5$, $\rho = 2$, $\theta_{\text{in}} = \pi/2$. The other parameter values are as follows: (*a*) $\chi_1^{(2)} \neq 0$, $\chi_{2-4}^{(2)} = 0$, $\sigma = 0.5$, $\varphi_{\text{in}} = \pi/4$, (*b*) $\chi_1^{(2)} \neq 0$, $\chi_{2-4}^{(2)} = 0$, $\sigma = 0.5$, $\varphi_{\text{in}} = \pi/2$, (*c*) $\chi_4^{(2)} \neq 0$, $\chi_{1-3}^{(2)} = 0$, $\sigma = 0$, $\varphi_{\text{in}} = 0$, (*d*) $\chi_4^{(2)} \neq 0$, $\chi_{1-3}^{(2)} = 0$, $\sigma = 0$, $\varphi_{\text{in}} = \pi/4$, (*e*) $\chi_4^{(2)} \neq 0$, $\chi_{1-3}^{(2)} = 0$, $\sigma = 0$, $\varphi_{\text{in}} = \pi/2$. The legend is shown in panel *f*.

parameters ($\forall\theta_{\text{in}}, \forall\varphi_{\text{in}}, \forall\sigma$):

$$\mathbf{f}^{(2\omega)}(\theta, -\varphi) = (1 - 2\mathbf{e}_\varphi \otimes \mathbf{e}_\varphi)\mathbf{f}^{(2\omega)}(\theta, \varphi),$$
$$\mathrm{Re}\left[\mathbf{f}^{(2\omega)}(\theta, \varphi)\right] = 0,$$
$$S_r^{(2\omega)}(\theta, -\varphi) = S_r^{(2\omega)}(\theta, \varphi). \quad (7)$$

The first and the third properties in formulae (7) are manifested in directivity patterns as a mirror symmetry plane that passes through the particle symmetry axis and the wave vector of an incident electromagnetic wave. This applies to Fig. 2, *b* and Figs. 5, *c, d*.

When the wave vector of excitation radiation is perpendicular to the symmetry axis of an ellipsoidal particle ($\theta_{\text{in}} = \pi/2$) and the other parameters assume arbitrary values ($\forall\chi_{1-4}^{(2)}, \forall\varphi_{\text{in}}, \forall\sigma$), the following properties are valid:

$$\mathbf{f}^{(2\omega)}(\theta, -\varphi) = -(1 - 2\mathbf{e}_r \otimes \mathbf{e}_r)\mathbf{f}^{(2\omega)}(\pi - \theta, \varphi),$$
$$S_r^{(2\omega)}(\theta, -\varphi) = S_r^{(2\omega)}(\pi - \theta, \varphi). \quad (8)$$

The spatial distribution of generated radiation features a twofold rotation axis of symmetry, which is parallel to the wave vector of an incident wave, in this case. Such features are apparent in the directivity patterns in Figs. 2–5, 7 and Fig. 6, *d*.

When a major or minor semiaxis of the polarization ellipse is perpendicular to the dielectric particle axis ($\varphi_{\text{in}} = \pi m/2$), the following relations hold true at any values of the other parameters ($\forall\chi_{1-4}^{(2)}, \forall\sigma$):

$$i\mathbf{f}^{(2\omega)}(\theta, -\varphi) = \left[i(1 - 2\mathbf{e}_\varphi \otimes \mathbf{e}_\varphi)\mathbf{f}^{(2\omega)}(\theta, \varphi)\right]^*,$$
$$S_r^{(2\omega)}(\theta, -\varphi) = S_r^{(2\omega)}(\theta, \varphi). \quad (9)$$

They are associated with the mirror symmetry of directivity patterns with respect to a plane passing through the wave vector of an incident electromagnetic wave and the particle axis. The indicated features are discernible in the directivity patterns in Figs. 2–6 and Figs. 7, *b, c, e*.

If a nonlinear layer covering a spheroidal particle does not have chiral properties ($\chi_4^{(2)} = 0$) and condition $\varphi_{\text{in}} = \pi m/4$ is satisfied, the following is true at arbitrary values of the other parameters ($\forall\chi_{1-3}^{(2)}, \forall\theta_{\text{in}}, \forall\sigma$):

$$\mathrm{Re}\left[\mathbf{f}^{(2\omega)}(\theta, -\varphi)\exp\left(i(m+1)\pi/2\right)\right] = \mathrm{Re}\left[(1 - 2\mathbf{e}_\varphi \otimes \mathbf{e}_\varphi)\mathbf{f}^{(2\omega)}(\theta, \varphi)\exp\left(i(m+1)\pi/2\right)\right]. \quad (10)$$

This feature is not manifested in any way in directivity patterns of generated radiation and characterizes the phase specifics of generated electromagnetic waves.

Function $\mathbf{f}^{(2\omega)}(\theta, \varphi)$ for a layer without chiral properties ($\chi_4^{(2)} = 0$) assumes only imaginary values under linear polarization of excitation radiation ($\sigma = 0$) and any values of the other parameters ($\forall\chi_{1-3}^{(2)}, \forall\theta_{\text{in}}, \forall\varphi_{\text{in}}$):

$$\mathrm{Re}\left[\mathbf{f}^{(2\omega)}(\theta, \varphi)\right] = 0. \quad (11)$$

This has already been noted earlier in the studies into generation in the surface layer of spherical [3] and cylindrical [2] particles.

If a layer has chiral properties only ($\forall\chi_4^{(2)}, \chi_{1-3}^{(2)} = 0$) and an incident wave is linearly polarized ($\sigma = 0$), the following equality is satisfied:

$$\mathrm{Im}\left[\mathbf{f}^{(2\omega)}(\theta, \varphi)\right] = 0. \quad (12)$$

The next set of relations holds true in the case of incidence of electromagnetic waves along the axis of an ellipsoidal particle ($\theta_{\text{in}} = 0, \pi, \forall\chi_{1-4}^{(2)}, \forall\varphi_{\text{in}}, \forall\sigma$):

$$\mathbf{f}^{(2\omega)}(-\theta, \varphi) = -(1 - 2\mathbf{e}_r \otimes \mathbf{e}_r)\mathbf{f}^{(2\omega)}(\theta, \varphi + \pi m),$$
$$\mathrm{Im}\left[\left(1 - (1-i)\mathbf{e}_\varphi \otimes \mathbf{e}_\varphi\right)\mathbf{f}^{(2\omega)}\left(\theta, \frac{\pi m}{2} + (-1)^{\frac{\theta_{\text{in}}}{\pi}}\varphi_{\text{in}} - \varphi\right) \times \exp(im\pi/2)\right] = \mathrm{Im}\left[\left(1 - (1-i)\mathbf{e}_\varphi \otimes \mathbf{e}_\varphi\right) \times \mathbf{f}^{(2\omega)}\left(\theta, (-1)^{\frac{\theta_{\text{in}}}{\pi}}\varphi_{\text{in}} + \varphi\right)\exp(im\pi/2)\right],$$
$$i\left(1 - (1-i)\mathbf{e}_\varphi \otimes \mathbf{e}_\varphi\right)\mathbf{f}^{(2\omega)}\left(\theta, \pi m - \varphi + (-1)^{\theta_{\text{in}}/\pi}\varphi_{\text{in}}\right) = \left[i\left(1 - (1-i)\mathbf{e}_\varphi \otimes \mathbf{e}_\varphi\right)\mathbf{f}^{(2\omega)}\left(\theta, \varphi + (-1)^{\theta_{\text{in}}/\pi}\varphi_{\text{in}}\right)\right]^*,$$
$$S_r^{(2\omega)}(-\theta, \varphi) = S_r^{(2\omega)}(\theta, \varphi + \pi m),$$
$$S_r^{(2\omega)}\left(\theta, \pi m - \varphi + (-1)^{\theta_{\text{in}}/\pi}\varphi_{\text{in}}\right) = S_r^{(2\omega)}\left(\theta, \varphi + (-1)^{\theta_{\text{in}}/\pi}\varphi_{\text{in}}\right). \quad (13)$$

These features manifest themselves in directivity patterns as two mirror symmetry planes, both of which pass through the axis of the polarization ellipse and the particle symmetry axis (Figs. 6, *b, c, e*).

In the case of incidence of a circularly polarized electromagnetic wave ($\sigma = \pm 1$) along the symmetry axis of an ellipsoidal particle ($\theta_{\text{in}} = 0, \pi, \forall\chi_{1-4}^{(2)}, \forall\varphi_{\text{in}}$) the following is observed:

$$\mathbf{f}^{(2\omega)}(\theta, \varphi + \Delta\varphi) = \mathbf{f}^{(2\omega)}(\theta, \pi m + \varphi)\exp\left(i2\sigma(-1)^{\theta_{\text{in}}/\pi}\Delta\varphi\right),$$
$$i\left(1 - (1-i)\mathbf{e}_\theta \otimes \mathbf{e}_\theta\right)\mathbf{f}^{(2\omega)}(-\theta, \varphi) = \left[i\left(1 - (1-i)\mathbf{e}_\theta \otimes \mathbf{e}_\theta\right)\mathbf{f}^{(2\omega)}(\theta, \pi m - \varphi)\exp(4i\sigma\varphi_{\text{in}})\right]^*,$$
$$S_r^{(2\omega)}(\theta, \varphi + \Delta\varphi) = S_r^{(2\omega)}(\theta, \varphi),$$
$$S_r^{(2\omega)}(-\theta, \varphi) = S_r^{(2\omega)}(\theta, \pi m - \varphi), \quad (14)$$

where $\Delta\varphi$ is an arbitrary angle. These properties are represented in directivity patterns by a symmetry axis that

coincides with the symmetry axis of an ellipsoidal particle (Fig. 6, *c*).

At $\forall\chi_2^{(2)}, \chi_{1,3,4}^{(2)} = 0$, $\forall\sigma$, and $\forall\varphi_{\text{in}}$ with the wave vector of an incident wave being aligned with the particle axis ($\theta_{\text{in}} = 0,\ \pi$), the following equalities are satisfied:

$$\mathbf{e}_\varphi \mathbf{f}^{(2\omega)}(\theta, \varphi) = 0,$$

$$\mathbf{f}^{(2\omega)}(\theta, \varphi + \Delta\varphi) = \mathbf{f}^{(2\omega)}(\theta, \varphi),$$

$$S_r^{(2\omega)}(\theta, \varphi + \Delta\varphi) = S_r^{(2\omega)}(\theta, \varphi). \quad (15)$$

They are manifested in the form of axial symmetry of the directivity pattern with a symmetry axis directed along the one of an ellipsoidal particle.

In a non-chiral layer ($\chi_4^{(2)} = 0,\ \forall\chi_{1-3}^{(2)},\ \forall\theta_{\text{in}},\ \forall\varphi_{\text{in}},\ \forall\sigma$) with excitation radiation propagating along the axis of a spheroidal particle, relations

$$\text{Re}\left[\mathbf{f}^{(2\omega)}(\theta, \varphi + \pi m/2 + \pi/2)\right] = -(-1)^m \text{Re}[\mathbf{f}^{(2\omega)}(\theta, \varphi)], \quad (16)$$

which characterize the specifics of variation of phase of generated radiation induced by a $\pi/2$ shift of the observation angle, are satisfied.

Likewise, in a chiral layer ($\chi_4^{(2)} \neq 0,\ \forall\chi_{1-3}^{(2)} = 0,\ \forall\theta_{\text{in}}$, $\forall\varphi_{\text{in}},\ \forall\sigma$) with an incident electromagnetic wave propagating in the same direction, equality

$$\text{Im}\left[\mathbf{f}^{(2\omega)}(\theta, \varphi + \pi m + \pi/2)\right] = -\text{Im}\left[\mathbf{f}^{(2\omega)}(\theta, \varphi)\right], \quad (17)$$

which is associated with the phase properties of second-harmonic radiation, holds true.

Properties associated with parameter substitution

Additional properties of functions $\mathbf{f}^{(2\omega)}$ and $S_r^{(2\omega)}$ become apparent following the substitution of certain parameters of the problem. New values of parameters and functions, which depend on these new parameters, are denoted by a tilde (e.g., $\tilde{\mathbf{f}}^{(2\omega)}$ and $\tilde{S}_r^{(2\omega)}$).

Property 1. The substitution of polarization with an opposite one ($\tilde{\sigma} = -\sigma$) in the case of generation in a non-chiral layer ($\chi_{1-3}^{(2)} \neq 0,\ \chi_4^{(2)} = 0$) yields the following:

$$i\tilde{\mathbf{f}}^{(2\omega)}(\theta, \varphi) = -\left[i\mathbf{f}^{(2\omega)}(\theta, \varphi)\right]^*,$$

$$\tilde{S}_r^{(2\omega)}(\theta, \varphi) = S_r^{(2\omega)}(\theta, \varphi). \quad (18)$$

Property 2. If the polarization sign is changed ($\tilde{\sigma} = -\sigma$) at $\chi_4^{(2)} \neq 0,\ \chi_{1-3}^{(2)} = 0$, the following equalities are satisfied:

$$\tilde{\mathbf{f}}^{(2\omega)}(\theta, \varphi) = \left[\mathbf{f}^{(2\omega)}(\theta, \varphi)\right]^*,$$

$$\tilde{S}_r^{(2\omega)}(\theta, \varphi) = S_r^{(2\omega)}(\theta, \varphi). \quad (19)$$

Properties 1 and 2 imply that a change in ellipticity of excitation radiation leads to a similar ellipticity reversal for generated radiation. In analytical terms, these features are attributable to an accompanying substitution of vector $\mathbf{e}^{(2\omega)}$, which characterizes the polarization of excitation radiation, with a complex conjugate one: $\tilde{\mathbf{e}}^{(2\omega)} = [\mathbf{e}^{(2\omega)}]^*$. These properties are illustrated by the directivity patterns in Fig. 3, *d*, Fig. 4, *c*, and Figs. 4, *e,f*.

Property 3. The following properties emerge upon symmetric reflection of the polarization ellipse of excitation radiation with respect to incidence plane *OXZ* ($\tilde{\varphi}_{\text{in}} = -\varphi_{\text{in}}$) or upon the $\tilde{\varphi}_{\text{in}} = \pi - \varphi_{\text{in}}$ substitution (reflection of the polarization ellipse with respect to the plane in which wave vector $\mathbf{k}^{(\omega)}$ of an incident wave and axis *OY* lie):

$$i\tilde{\mathbf{f}}^{(2\omega)}(\theta, \varphi) = \left[i(1 - 2\mathbf{e}_\varphi \otimes \mathbf{e}_\varphi)\mathbf{f}^{(2\omega)}(\theta, -\varphi)\right]^*,$$

$$\tilde{S}_r^{(2\omega)}(\theta, \varphi) = S_r^{(2\omega)}(\theta, -\varphi). \quad (20)$$

This is manifested in the spatial distribution of generated radiation as a reflection of the directivity pattern with respect to the incidence plane.

Property 4. The following equalities hold true in the case of reflection of the wave vector with respect to plane *OXY*, which is perpendicular to the incidence plane:

$$\tilde{\mathbf{f}}^{(2\omega)}(\theta, \varphi) = -(1 - 2\mathbf{e}_r \otimes \mathbf{e}_r)\mathbf{f}^{(2\omega)}(\pi - \theta, -\varphi),$$

$$\tilde{S}_r^{(2\omega)}(\theta, \varphi) = S_r^{(2\omega)}(\pi - \theta, -\varphi). \quad (21)$$

This reflection corresponds to substitution $\tilde{\theta}_{\text{in}} = \pi - \theta_{\text{in}}$, which induces a rotation of the directivity pattern of generated radiation by π about axis *OX* that lies within the incidence plane and is perpendicular to the particle axis.

No-generation conditions

Generation of radiation in the surface layer of an ellipsoidal particle does not occur under certain values of the problem parameters. In mathematical terms, this is represented as $\mathbf{f}^{(2\omega)}(\theta, \varphi) = 0$. Similar conditions have been determined earlier in the analysis of second-harmonic generation and sum-frequency generation in surface layers of spherical [3] and cylindrical [9] particles.

(1) In the case of generation in the directions where $q_\perp(\mathbf{x}) = 0$ or $q_z(\mathbf{x}) = 0$, certain components of integrals $I(n_i|\mathbf{x})$, $I(n_i n_j|\mathbf{x})$, and $I(n_i n_j n_k|\mathbf{x})$ turn to zero. If conditions $q_\perp(\mathbf{x}) = 0$ and $q_z(\mathbf{x}) = 0$ are satisfied simultaneously (i.e., $\mathbf{q} = 0$), generation due to non-chiral components $\chi_{1-3}^{(2)}$ is lacking (this has already been noted in [2,3,10]). If a particle and the environment are dispersionless ($\xi = 1$), the scattering vector is zero in the direction coinciding with the orientation of the wave vector of an incident wave. Therefore, generation in this direction is lacking at $\forall\chi_{1-3}^{(2)}, \chi_4^{(2)} = 0$. If the value of coefficient ξ is close to unity, radiation in the direction of the wave vector of an incident electromagnetic wave is generated, but the intensity of the second harmonic is very low, since $|\mathbf{q}|a_x \ll 1$. The

fulfillment of such conditions is illustrated by the directivity patterns in Figs. 2, *a–c, e*, Figs. 3–6, and Figs. 7, *a, b*.

Importantly, this property may be used to determine the chiral component of tensor $\chi^{(2)}_{ijk}$ by measuring the radiation power density in the direction coinciding with the orientation of the wave vector of an incident electromagnetic wave. Generation is then maintained primarily by component $\chi^{(2)}_4$.

(2) When an electromagnetic wave is incident along the axis of an ellipsoidal particle ($\theta_{\text{in}} = 0,\ \pi$), generation in the directions parallel to the particle axis ($\theta = 0, \pi, \forall\varphi$) is suppressed at any particle size ($\forall a_x, \forall\rho$), any values of independent components of the tensor of nonlinear dielectric susceptibility ($\forall\chi^{(2)}_{1-4}$), and any polarization of excitation radiation ($\forall\varphi_{\text{in}}, \forall\sigma$). The indicated property is manifested in the directivity patterns in Figs. 6, *b, c, f*.

(3) If the only nonzero component of the tensor of nonlinear dielectric susceptibility is $\chi^{(2)}_2$ ($\chi^{(2)}_{1,3,4} = 0,\ \chi^{(2)}_2 \neq 0$), second-harmonic radiation is not generated by an ellipsoidal particle under excitation with circularly polarized radiation ($|\sigma| = 1$). The other parameters may assume arbitrary values in this case ($\forall a_x, \forall\rho, \forall\theta_{\text{in}}, \forall\varphi_{\text{in}}, \forall\theta, \forall\varphi$).

Circularly polarized excitation radiation may be useful if one is to avoid the influence of component $\chi^{(2)}_2$ on generation (for measuring the other components). Specifically, this component is dominant for malachite green dye [6] and shapes the directivity pattern under linear polarization of excitation radiation.

(4) When the wave vector of an incident electromagnetic wave is directed perpendicular to the particle axis ($\theta_{\text{in}} = \pi/2$), generation is not observed in the directions parallel to this wave vector ($\theta = \pi/2$). No restrictions are imposed on the other problem parameters ($\forall\chi^{(2)}_{1-4}, \forall a_x, \forall\rho, \forall\sigma, \forall\varphi_{\text{in}}, \forall\varphi$). This feature is illustrated by the directivity patterns in Figs. 2–5, 7 and Fig. 6, *d*.

(5) At $\chi^{(2)}_3 \neq 0$, $\chi^{(2)}_{1,2,4} = 0$, generation does not occur in plane OXY ($\theta = \pi/2, \forall\varphi$) in the case of irradiation of a spheroidal dielectric particle of an arbitrary size ($\forall a_x, \forall\rho$) with a linearly polarized wave ($\sigma = 0$) if the wave vector of excitation radiation is perpendicular to the particle axis ($\theta_{\text{in}} = \pi/2$) and the electric field vector of double-frequency radiation is directed along the particle axis ($\varphi_{\text{in}} = 0,\ \pi$). An example of the corresponding directivity pattern is provided by Fig. 3, *d*.

(6) If the values of components of the tensor of nonlinear dielectric susceptibility are $\chi^{(2)}_3 \neq 0,\ \chi^{(2)}_{1,2,4} = 0$, generation is not observed (Fig. 4, *d*) in the directions with $\theta = \pi/2,\ \varphi = m_2\pi/2$ in the case of incidence of linearly polarized excitation radiation ($\sigma = 0$) with any semiaxis of its polarization ellipse being perpendicular to the particle axis ($\varphi_{\text{in}} = m_1\pi/2$). The other parameters may assume arbitrary values ($\forall a_x, \forall\rho, \forall\theta_{\text{in}}$).

(7) A chiral surface layer ($\chi^{(2)}_4 \neq 0,\ \chi^{(2)}_{1-3} = 0$) of a dielectric spheroidal particle of an arbitrary size ($\forall a_x, \forall\rho$) has zero generation in the plane perpendicular to the particle axis ($\theta = \pi/2, \forall\varphi$) if the wave vector of a linearly polarized ($\sigma = 0$) electromagnetic wave is perpendicular to the particle axis ($\theta_{\text{in}} = \pi/2$), which, in turn, lies in the polarization plane of excitation radiation ($\varphi_{\text{in}} = 0,\ \pi$).

(8) A chiral layer ($\chi^{(2)}_4 \neq 0,\ \chi^{(2)}_{1-3} = 0$) also features suppressed generation in plane OXZ ($\forall\theta,\ \varphi = 0,\ \pi$) if an incident electromagnetic wave is linearly polarized ($\sigma = 0$) and its polarization plane is perpendicular to the particle axis ($\varphi_{\text{in}} = \pm\pi/2$). The other parameters may assume arbitrary values ($\forall a_x, \forall\rho, \forall\theta_{\text{in}}$). This property is illustrated by Fig. 7, *e*.

(9) Generation in the directions parallel to the particle axis ($\theta = 0, \pi, \forall\varphi$) is also lacking when the wave vector of a linearly polarized incident electromagnetic wave is perpendicular to the particle axis ($\theta_{\text{in}} = \pi/2$) and either one of the semiaxes of the polarization ellipse is aligned with the particle axis ($\varphi_{\text{in}} = m\pi/2$). The requirements imposed on independent components of the tensor of nonlinear dielectric susceptibility are $\chi^{(2)}_3 \neq 0,\ \forall\chi^{(2)}_{1,2,4}$ (Fig. 4, *d*). A particle may have arbitrary linear dimensions in this case ($\forall a_x, \forall\rho$).

(10) Second-harmonic generation is also not observed in the directions perpendicular to the polarization plane ($\forall\theta,\ \varphi = \pm\pi/2 + (-1)^{\theta_{\text{in}}/\pi}\varphi_{\text{in}}$) of a linearly polarized ($\sigma = 0$) incident electromagnetic wave if only the third independent component of the tensor of nonlinear dielectric susceptibility is nonzero ($\chi^{(2)}_{1,2,4} = 0,\ \chi^{(2)}_3 \neq 0$) and the wave vector of an incident wave is aligned with the particle symmetry axis ($\theta_{\text{in}} = 0,\ \pi$). The other parameters have no effect on the result ($\forall a_x, \forall\rho, \forall\varphi_{\text{in}}$). The directivity pattern illustrating this case is shown in Fig. 4, *d*.

Condition (10) may be applied, e.g., in those cases when the influence of component $\chi^{(2)}_3$ on generation needs to be suppressed for the measurement of other components. The procedure of determination of components of tensor $\chi^{(2)}_{ijk}$ with the use of no-generation conditions was detailed in studies [3] and [9] focused on generation in the surface layer of spherical and cylindrical dielectric particles, respectively.

Conditions for generation of linearly polarized radiation

In addition to establishing no-generation conditions, specific combinations of problem parameters may be used to generate linearly polarized radiation. The mathematical criterion for linear polarization of generated radiation is as follows:

$$\text{Re}\left[(\mathbf{f}^{(2\omega)}\mathbf{e}_\theta)^*(\mathbf{f}^{(2\omega)}\mathbf{e}_\varphi)\right] = 0. \tag{22}$$

The fulfillment of this condition implies that vector $\mathbf{f}^{(2\omega)}$ has matching phases of components along vectors $\mathbf{e}_\theta$ and $\mathbf{e}_\varphi$. Oscillations of the electric field vector of double-frequency radiation then proceed along vector

$$\mathbf{e}_\theta|\mathbf{e}_\theta\mathbf{f}^{(2\omega)}| + \mathbf{e}_\varphi|\mathbf{e}_\varphi\mathbf{f}^{(2\omega)}|. \tag{23}$$

The conditions under which linearly polarized radiation is generated have been formulated earlier in [3,9] in the

context of second-harmonic generation in spherical and cylindrical dielectric particles, respectively.

(1) When a spheroidal dielectric particle is subjected to incident linearly polarized radiation ($\sigma = 0$), the polarization of generated second-harmonic radiation is also linear if the optically nonlinear layer is not chiral ($\chi^{(2)}_{1-3} \neq 0$, $\chi^{(2)}_4 = 0$, $\forall a_x$, $\forall\rho$, $\forall\theta_{\text{in}}$, $\forall\varphi_{\text{in}}$). This property is manifested in Figs. 4, *a, d* and is a corollary of property (11) under which criterion (22) is satisfied.

(2) If a linearly polarized electromagnetic wave ($\sigma = 0$) is incident on a particle shaped as an ellipsoid of revolution, linearly polarized radiation is generated only when the layer features strictly chiral properties ($\chi^{(2)}_4 \neq 0$, $\chi^{(2)}_{1-3} = 0$, $\forall a_x$, $\forall\rho$, $\forall\theta_{\text{in}}$, $\forall\varphi_{\text{in}}$). This is illustrated by Figs. 7, *c–f*. Linearly polarized radiation is generated in this case due to the fulfillment of condition (12), which implies that the phases of components of vector $\mathbf{f}^{(2\omega)}$ along vectors $\mathbf{e}_\theta$ and $\mathbf{e}_\varphi$ are matching.

(3) If $\chi^{(2)}_3 \neq 0$, $\forall\chi^{(2)}_2$, $\chi^{(2)}_{1,4} = 0$, an incident wave propagates along the particle symmetry axis ($\theta_{\text{in}} = 0,\ \pi$), and its polarization is circular ($|\sigma| = 1$), second-harmonic linearly polarized radiation is generated in the plane perpendicular to the particle symmetry axis ($\theta = \pi/2, \forall\varphi$; see Figs. 4, *e,f*). The values of the other parameters are irrelevant ($\forall a_x, \forall\rho, \forall\varphi_{\text{in}}$). Oscillations of the electric field vector of double-frequency radiation then proceed along vector $\mathbf{e}_\varphi$.

(4) If the only nonzero independent component of the tensor of nonlinear dielectric susceptibility is the second one ($\chi^{(2)}_2 \neq 0$, $\chi^{(2)}_{1,3,4} = 0$), second-harmonic linearly polarized double-frequency radiation is generated in all directions ($\forall\theta, \forall\varphi$) at $-1 < \sigma < 1$ and arbitrary values of the other parameters ($\forall a_x, \forall\rho, \forall\theta_{\text{in}}, \forall\varphi_{\text{in}}$; see Fig. 2, *b* and Figs. 5, *c, d*). This property is a corollary of (15).

(5) If the only nonzero independent component of tensor $\chi^{(2)}_{ijk}$ is the third one ($\chi^{(2)}_3 \neq 0$, $\chi^{(2)}_{1,2,4} = 0$), second-harmonic linearly polarized radiation is generated in the directions perpendicular to the particle axis ($\theta = \pi/2, \forall\varphi$) when the wave vector of an incident electromagnetic wave is aligned with the particle symmetry axis ($\theta_{\text{in}} = 0,\ \pi$). The electric field vector of the second harmonic then oscillates the oscillates along vector $\mathbf{e}_\varphi$.

The conditions for generation of linearly polarized radiation may be used to determine and clarify the values of individual components of the tensor of nonlinear dielectric susceptibility. For example, if the third combination of conditions specified in this section ($|\sigma| = 1,\ \theta = \pi/2$, $\forall\varphi, \forall a_x, \forall\rho, \forall\varphi_{\text{in}}$) is satisfied, the component of the generated electric field vector directed along $\mathbf{e}_\theta$ depends only on coefficient $\chi^{(2)}_1$ (if the layer does not feature chiral properties, $\chi^{(2)}_4 = 0$). The application of such conditions in the determination of coefficients $\chi^{(2)}_{1-4}$ was discussed in more detail in [3,9].

Conclusion

The primary reason for conducting an in-depth analysis of cases with a simplified tensor of nonlinear dielectric susceptibility (with only one of its independent components being nonzero) consists in the fact that the properties of the spatial distribution of generated radiation (symmetry property,no-generation condition, condition for generation of linearly polarized radiation) are the most strongly pronounced and exposed to analytical characterization in these cases.

However, the obtained results may also find application in analysis of the spatial distribution of generated radiation with a real tensor:

— if one of its independent components is significantly larger in absolute value than the others;

— if several dominant components of this tensor have a certain common feature. A feature typical of the corresponding simplified tensor should then be manifested in the directivity pattern for a real tensor.

The parameters of the problem used in calculation of components of the electric field of the second harmonic affect directly the nature of the spatial distribution of generated radiation in the far-field region. In the case of a small dielectric particle, each non-chiral component $\chi^{(2)}_{1-3}$ of the tensor of nonlinear dielectric susceptibility has its own shape of the directivity pattern. The directivity pattern for chiral component $\chi^{(2)}_4$ is similar in shape to the pattern for $\chi^{(2)}_2$ corresponding to coefficient ρ values differing considerably from unity. This has not been observed earlier in generation in the surface layer of a spherical dielectric particle.

The ratio of semiaxes of the polarization ellipse of an incident wave affects directly the polarization of double-frequency radiation and specifies explicitly the direction in which the generated second-harmonic radiation power is higher.

The incidence of linearly polarized electromagnetic waves on a spheroidal dielectric particle coated with an optically nonlinear layer induces generation of linearly polarized radiation if the surface layer is chiral ($\chi^{(2)}_4 \neq 0$, $\chi^{(2)}_{1-3} = 0$) or non-chiral ($\chi^{(2)}_{1-3} \neq 0$, $\chi^{(2)}_4 = 0$). Elliptically or circularly polarized incident waves induce generation of elliptically polarized radiation. When the polarization of excitation radiation switches to an opposite one, the polarization of generated radiation also reverses, while the amplitude remains the same.

In the case of proportional scaling of linear dimensions of a spheroidal dielectric particle, up to two preferred radiation directions typically emerge in the directivity pattern for second-harmonic radiation.

A rotation of the wave vector of an incident electromagnetic wave and its polarization ellipse induce a corresponding rotation of the main lobes of the directivity pattern and a redistribution of the generated radiation power density between them.

The symmetry properties revealed in the directivity patterns of double-frequency radiation are related to the mathematical properties of functions characterizing the spatial distribution of generated radiation. The determined mathematical properties specify the symmetry of spatial distribution of generated radiation and are indicative of the trends in variation of phase and amplitude characteristics of generated radiation, which are observed when the problem parameters are varied. Each independent component of the tensor of nonlinear dielectric susceptibility has its own set of features that are associated, for illustrative purposes, with the directivity patterns of double-frequency radiation. These features may be used to determine tentatively the dominant component of tensor $\chi^{(2)}_{ijk}$ by analyzing the shape of the directivity pattern.

The conditions for generation of linearly polarized radiation and no-generation conditions (alongside with the mathematical properties) characterize the specifics of the spatial distribution of generated radiation typical of each coefficient $\chi^{(2)}_{1-4}$. These conditions may be used efficiently to determine individual components of the tensor of nonlinear dielectric susceptibility by suppressing the influence of the other components on the distribution pattern of generated radiation.

Funding

This study was supported financially by the Belarusian Republican Foundation for Fundamental Research (grant F20M−011).

Conflict of interest

The authors declare that they have no conflict of interest.

References

[1] A.A. Shamyna, V.N. Kapshai. Opt. Spectrosc., **126** (6), 645 (2019). DOI: 10.1134/S0030400X19060225.
[2] V.N. Kapshai, A.A. Shamyna. Opt. Spectrosc., **126** (6), 653 (2019). DOI: 10.1134/S0030400X19060134.
[3] V.N. Kapshai, A.A. Shamyna. Opt. Spectrosc., **123** (3), 440 (2017). DOI: 10.1134/S0030400X17090144.
[4] A.A. Shamyna, V.N. Kapshai. Opt. Spectrosc., **124** (1), 103 (2018). DOI: 10.1134/S0030400X18010198.
[5] A.A. Shamyna, V.N. Kapshai. Opt. Spectrosc., **125** (1), 71 (2018). DOI: 10.1134/S0030400X1807024X.
[6] S. Wunderlich, B. Schürer, C. Sauerbeck, W. Peukert, U. Peschel. Phys. Rev. B, **84** (23), 235403 (2011). DOI: 10.1103/PhysRevB.84.235403
[7] S. Viarbitskaya, V. Kapshai, P. van der Meulen, T. Hansson. Phys. Rev. A, **81** (5), 053850 (2010). DOI: 10.1103/PhysRevA.81.053850
[8] S. Jen, H. Dai, G. Gonella. J. Phys. Chem. C, **114** (10), 4302 (2010). DOI: 10.1021/jp910144c
[9] A.A. Shamyna, V.N. Kapshai. Opt. Spectrosc., **126** (6), 661 (2019). DOI: 10.1134/S0030400X19060237.
[10] J.I. Dadap, J. Shan, T. Heinz. J. Opt. Soc. Am. B., **21** (7), 1328 (2004). DOI: 10.1364/JOSAB.21.001328